STUDIES ON THE MECHANISM OF ASSEMBLY OF TOBACCO MOSAIC VIRUS

Todd M. Schuster, Robert B. Scheele, Mary L. Adams, Steven J. Shire, John J. Steckert, and Martin Potschka, *Biochemistry and Biophysics Section, Biological Sciences Group, University of Connecticut, Storrs, Connecticut 06268 U.S.A.*

ABSTRACT Sedimentation and proton binding studies of the endothermic self-association of tobacco mosaic virus (TMV) protein indicate that the so-called "20S" sedimenting protein is an interaction system involving at least the 34-subunit two-turn cylindrical disk aggregate and the 49-subunit three-turn helical rod. The pH dependence of this overall equilibrium suggests that disk formation is proton-linked through the binding of protons to the two-turn helix which is not present at significant concentrations near pH 7. There is a temperature-induced intramolecular conformation change in the protein leading to a difference spectrum which is complete in 5×10^{-6} s at pH 7 and 20°C and is dominated at 300 nm by tryptophan residues. Kinetics measurements of protein polymerization, from 10^{-6} to 10^{3} s, reveal three relaxation processes at pH 7.0, 20°C, 0.10 M ionic strength $K(H)PO_4$. The fastest relaxation time is a few milliseconds and represents reactions within the 4S protein distribution. The second fastest relaxation is $50–100 \times 10^{-3}$ s and represents elementary polymerization steps involved in the formation of the ~20S protein. Analysis of the slowest relaxation, $\sim 5 \times 10^{4}$ s, suggests that this very slow formation of ~20S protein may be dominated by some first order process in the overall dissociation of ~20S protein. Sedimentation measurements of the rate of TMV reconstitution, under the same conditions, show by direct measurements of 4S and ~20S incorporation at various 4S to ~20S weight ratios that the relative rate of ~20S incorporation decreases almost linearly, from 0 to 50% 4S. There appears to be one or more regions of TMV-RNA, ~1–1.5 kilobases long, which incorporates ~20S protein exclusively. Solutions of ~95–100% ~20S protein have been prepared for the first time and used for reconstitution with RNA. Such protein solutions yield full size TMV, but at a slower rate than if 4S protein is added. Thus the elongation reaction in TMV assembly, following nucleation with ~20S protein, is not exclusively dependent upon the presence of either 4S or ~20S protein aggregates. The initial, maximum, rate of reconstitution increases about threefold when the protein composition is changed from 5% to 30% 4S protein, at constant total protein concentration at pH 7.0, 20°C in 0.10 M ionic strength $K(H)PO_4$. The probable binding frame at the internal assembly nucleation site of TMV-RNA has been determined by measuring the association constants for the binding of various trinucleoside diphosphates to helical TMV protein rods. The -CAG-AAG-AAG-sequence at the nucleation site is capable of providing at least 10–14 kcal/mol of sites of binding free energy for the nucleation event in TMV self-assembly.

INTRODUCTION

The self-assembly of tobacco mosaic virus (TMV) from its components (1) results from specific protein-protein and protein-nucleic acid interactions. To a good approximation these interactions can be studied separately, since the coat protein alone (TMVP) can be made to

---

Dr. Schuster is a McCollum-Pratt Fellow, 1979-1980, of the McCollum-Pratt Institute, The Johns Hopkins University, Baltimore, Md. 21218.

Dr. Scheele's present address is Molecular Biology Laboratory, University of Wisconsin, Madison, Wis. 53706.

form virus-like helical rods (for reviews, see references 2 and 3). In this paper we report the results of recent studies aimed at understanding the dynamics of these interactions and the detailed mechanism of TMV assembly. Recent reviews on the subject (4, 5, 6) also summarize progress on the x-ray diffraction elucidation of the structures of the coat protein (7) and of the virus (reference 8, Butler and Lomonosoff, these proceedings), as well as the sequence of the single RNA chain (reference 9, and Hirth et al., these proceedings).

PROTON-LINKED SELF-ASSOCIATION OF TMVP

Sedimentation and Proton Binding Measurements

The formation of helical rods from TMVP subunits is strongly endothermic (3) and involves many elementary steps (2), yet relatively few stable intermediate association states are observed. Although considerable effort has been devoted to the subject, a complete quantitative description of TMVP self-association is not available. Highly accurate equilibrium data have been obtained only for the very initial stages (monomer-trimer) of TMVP polymerization (10). However, it is known that the association of TMVP to form a ~20S sedimenting boundary is necessary for efficient reconstitution with RNA at pH 7, 20°C (11), as well as at pH 6.5, 6.5°C (12), conditions where TMV self-assembly has been most thoroughly characterized. The ~20S sedimenting boundary has been shown by electron microscopy to contain a 34 subunit (monomer = 17.5×10^3 d) aggregate of TMVP which has the form of a two-layer cylindrical disk similar in cross-sectional dimensions to the virus (13). The central role of this ~20S sedimenting boundary in virus reconstitution has been confirmed in several laboratories (4, 5, 6, 14, 15). The first step in TMVP and RNA assembly (nucleation) is thought to occur with the protein in the disk state. Some component of this same ~20S boundary can also act as the nucleating species involved in the formation of RNA-free helical TMVP rods (16, 17, 18).

Although the sedimentation coefficient of the "~20S" boundary depends upon protein concentration, pH, temperature, and ionic strength, exhibiting values from ~18–25S, there has been an uncritical assignment of this entire range of aggregation states to the two-layer disk. Closer examination of the pH dependence of the sedimentation coefficient at 20°C of the "disk" reveals an interestingly systematic change which is shown in the inset in Fig. 1 *a*. We have previously determined the 20°C intrinsic sedimentation coefficients, $s^\circ_{20,w}$, of this boundary at pH 7.0 and pH. 6.5, 20.4S and 24.4S, respectively, and provided evidence that the size of the major component in the pH 6.5, $s^\circ_{20,w}$ = 24.4S boundary is about a 49 subunit, three-turn short rod which is probably helical and corresponds to the smallest stable helical rod of TMVP (18). If the pH 7.0, $s^\circ_{20,w}$ = 20.4S boundary is predominantly a 34-subunit two-layer cylindrical disk (13), then the $s^\circ_{20,w}$ versus pH data in Fig. 1 *a* probably represents the overall equilibrium between these two forms:

$$H^+ + \text{two-turn disk} \underset{\longleftarrow}{\overset{K_1}{\longrightarrow}} \text{(two-turn helix)}$$

$$\text{(two-turn helix)} + \text{subunits} \underset{\longleftarrow}{\overset{K_2}{\longrightarrow}} \text{three-turn helix,}$$

the two-turn helix being unstable and present in very low concentrations.

Comparison of the ~19 to ~24S boundary with the extent of proton binding at the corresponding pH values is shown in Fig. 1 *a*. Cross plotting these data, as in Fig. 1 *b*, reveals a sharp increase in polymerization at ~0.1 H^+ bound per subunit. Subsequent H^+ binding

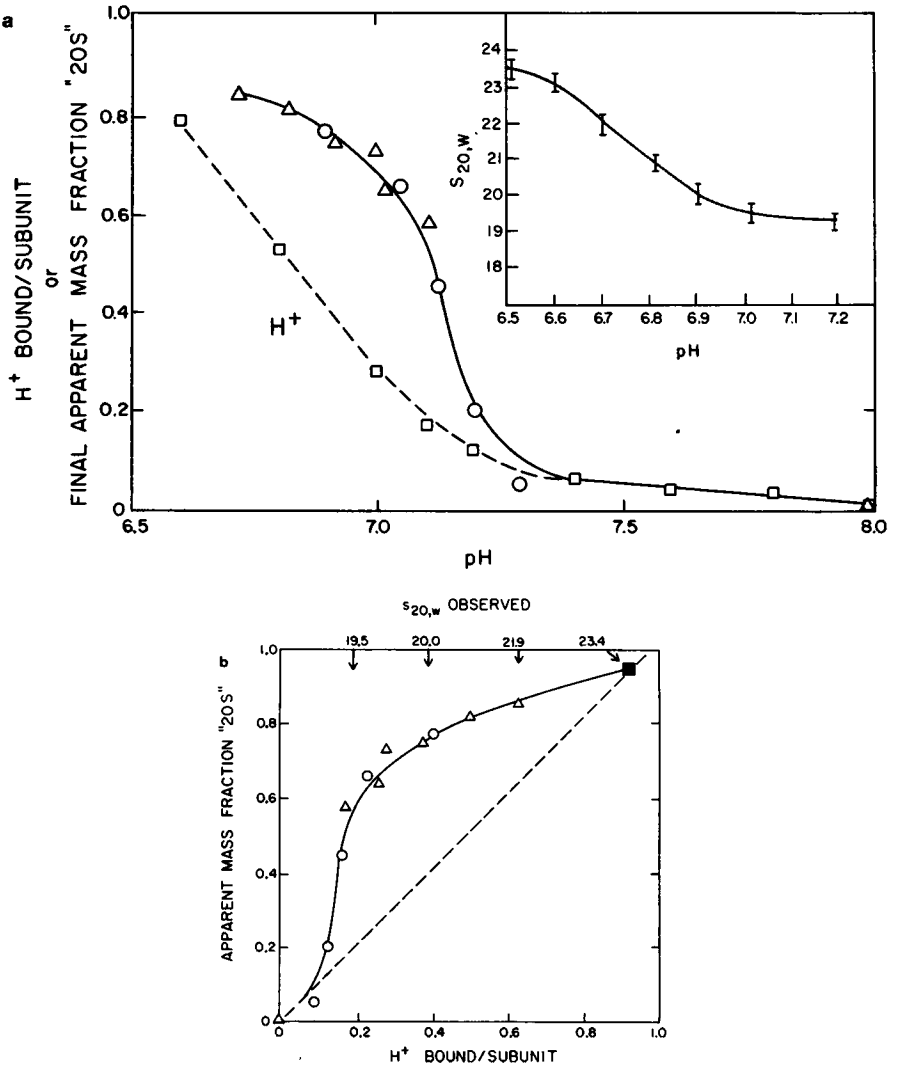

Figure 1 (*a*) pH dependence of the sedimentation coefficient of "20S" TMVP (inset) and of the corresponding mass fraction under final equilibrium conditions where there are only 4S and "20S" schlieren boundaries seen by analytical untracentrifugation. Δ, data from this study; O, data of Vogel and Jaenicke (20). Conditions, 0.10 M *I* K(H) PO_4, 5.0 mg ml^{-1}, 20°C. Details of protein preparation, ultracentrifugation, and special sample handling are given in references 17 and 18. Also shown is the number of protons bound per TMVP subunit at 20°C, relative to pH 8.0, □, taken from the data of Scheele and Lauffer (36) and corrected for hysteresis of proton binding as described by Scheele and Schuster (37). (*b*) Cross-plot of data from Fig. 1 *a*. plus one sedimentation datum, ■, from Shire, et. al., (18). Dashed line indicates unity slope expected if each subunit entering "20S" protein were to bind one proton.

appears to be more weakly coupled to polymerization, as is possible in the above scheme. This scheme is oversimplified in that at all equilibrium condtions where there is a ~19 to~24S boundary there is also present a slower sedimenting, ~4S, boundary which reflects a rapidly interacting self-association of subunits (monomer to trimer). These results suggest that it is mainly the helical rods which bind protons and that when the subunits are titrated to the

extent of an average of one polymerization-linked proton per subunit they polymerize into the smallest stable helical rod—a three-turn helix. It is known that at least one more proton per subunit can be bound at lower pH values, leading to the formation of long, virus-like helical rods, Shalaby and Lauffer (19) have also proposed that helical, but not disk, polymers bind protons, but their measured stoichiometry of proton binding differs from that shown in Fig. 1 *b* because of a different assignment of equilibrium states in analyzing TMVP titration curves. Vogel and Jaenicke (20) and Durham, et al. (21) have previously suggested that near pH 7 the disk aggregate is the proton binding species. However, in these studies it was apparently assumed that the entire range of ~19 to 24S boundaries represented the disk aggregate, which is clearly not the case. The present data are consistent with the idea that at pH7, 20°C, there are two charge states (conformations) of TMVP subunits (22) and raise the question of whether or not the formation of the disk is generally in the main kinetic reaction path leading to helical rods from subunits. Polymerization at 5°C and pH 5.5 appears not to proceed through the formation of disks (17).

Difference Spectroscopy

Direct evidence for polymerization-linked conformation changes in TMVP aggregates smaller than disk, ~4S, comes from measurements of the TMVP ultraviolet absorption spectrum as a function of temperature, concentration, pH, and, as shown previously by Vogel, from circular dichroism changes (20, 23). The temperature difference spectrum of TMVP shown in Fig. 2 *a* indicates contributions from phenylalanine, tyrosine, and tryptophan. Fig. 2 *b* shows dimethylsulfoxide induced red shift difference spectra of the N-acetyl, C-ethyl ester derivatives of these amino acids (24) scaled (see Fig. 2 *b*) according to the composition of these side chains in the interior of the protein as determined by x-ray crystallography (7). It appears that the extinction maxima of these amino acids in TMVP are significantly red-shifted from the model compounds even at 3.2°C, where at this pH and concentration TMVP is largely trimer and monomer (10). Raising the temperature to 13°C results in an increase in $\overline{M}w$ and, although there is no ~20S protein formed, the absorption bands are further red-shifted. Similar difference spectra, all dominated by tryptophan transitions, are obtained when $\overline{M}w$ is increased by concentration or pH changes. The temperature dependencies of $\Delta\epsilon_{300}$ and $\Delta\epsilon_{294}$, shown in Fig. 2 *c*, suggest that the former, which is dominated by tryptophan, represents a single spectral class of residues. However, at 294 nm both tyrosine and tryptophan transitions contribute to the difference spectrum, and above 21°C, where the ~20S boundary begins to form slowly, two classes of chromophores are evident. Up to 20°C, $\Delta\epsilon_{300}/\Delta\epsilon_{294} = 2.0\ (\pm 1)$ and, although this relation holds up to 28°C during the initial few minutes after slow temperature jumps (heating time 3 min), at longer times there is an enhanced contribution of tyrosine changes as ~20S protein forms. Separate experiments show that this slow change in $\Delta\epsilon_{294}$ parallels light-scattering changes which reflect ~20S formation. Under the conditions of Fig. 3 *a* $\Delta\epsilon_{294}(t)$ yields a value of $\sim 2.4 \times 10^{-5}\ s^{-1}$.

Kinetics of 4S and "20S" Formation and Dissociation

When the rate of the tryptophan spectral change was investigated at low protein concentrations (<1 mg ml^{-1}) by rapid temperature-jump methods it was found that the entire light-scattering-corrected equilibrium value of $\Delta\epsilon_{300}$ was obtained within the heating time of 5×10^{-6} s. Since at this protein concentration, $\sim 6 \times 10^{-5}$M monomer, a submicrosecond reaction is too fast to represent a bimolecular reaction between subunits, it can be assumed that this fast change in the protein extinction represents a temperature-dependent intramole-

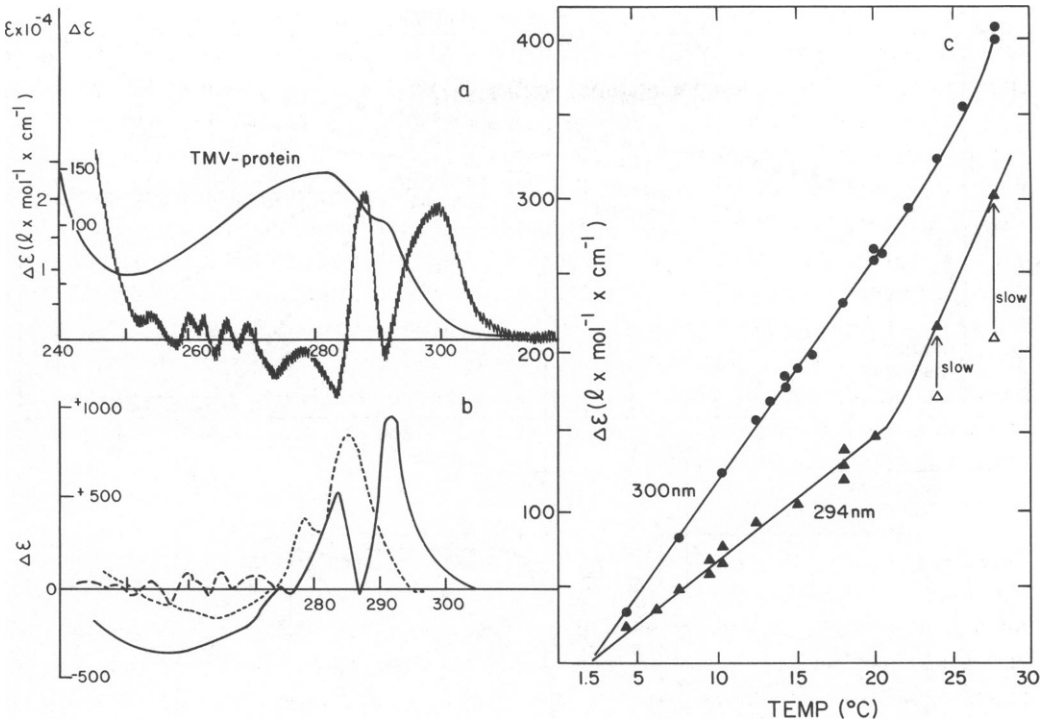

Figure 2 (*a*) Temperature-induced difference spectrum of TMVP, 12.8–3.2°C, 1.0 mg ml^{-1}, pH 6.03 at 20°C, 0.10 M *I* K(H)PO_4. No ~20S protein is present at either temperature and no time dependence was observed for $\Delta\epsilon$ values. Measurements were performed on a single sample scanned at each temperature at constant slit width such that one-half maximum bandwidth was always <0.7 nm, using a computer controlled Cary 118c spectrophotometer (Cary Instruments, Fairfield, N.J.) to acquire, average and store data. Spectra shown are not corrected for light-scattering. (*b*) Solvent (20% dimethysulfoxide, pH 6.8) induced difference spectra of isolated amino acid N-actyl, C-ethyl ester derivatives resulting from redshifts. Data taken from Herskovits (24) and scaled as follows: ——, 2 mol of tryptophan, ---, 8 mol phenylalanine, ..., 4 mol tyrosine. (*c*) Temperature dependence of difference spectrum in Fig. 2 *a*, same buffer, pH 7.02 at 20°C, 0.92 mg ml^{-1} TMVP. $\Delta\epsilon$ values scaled to 1.5°C but not corrected for light-scattering: ●, 300 nm; ▲, 294 nm; Δ, initial value at 294 nm after 3 min heating time temperature-jump from 1.5°C. See text for description of the origin of these changes. Lines have no theoretical meaning.

cular reaction. Furthermore, from chemical relaxation theory it can be shown that since this spectral shift indicates for the full time-course of ~20S formation, the reaction giving rise to this fast red-shift must be as fast as the fastest reaction step in the overall polymerization process. This result suggests that the kinetics of ~20S formation are not rate limited by this tryptophan conformation change. This very rapid temperature-induced conformation change may reflect the strongly endothermic elementary reaction within each TMVP subunit prior to aggregation which "drives" polymerization.

The overall kinetics of ~20S formation at 20°C as measured by slow temperature-jump light-scattering (Fig. 3 *a*) exhibit two apparent phases. The faster phase, which is complete within 10–15 min, is not measurable by sedimentation methods. The approach to final equilibrium takes many hundreds of minutes. Similarly long times for ~20S formation have been reported several times since the initial observation by Durham by using ultracentrifugation (25). However, no quantitative explanation for this very slow rate of ~20S formation has

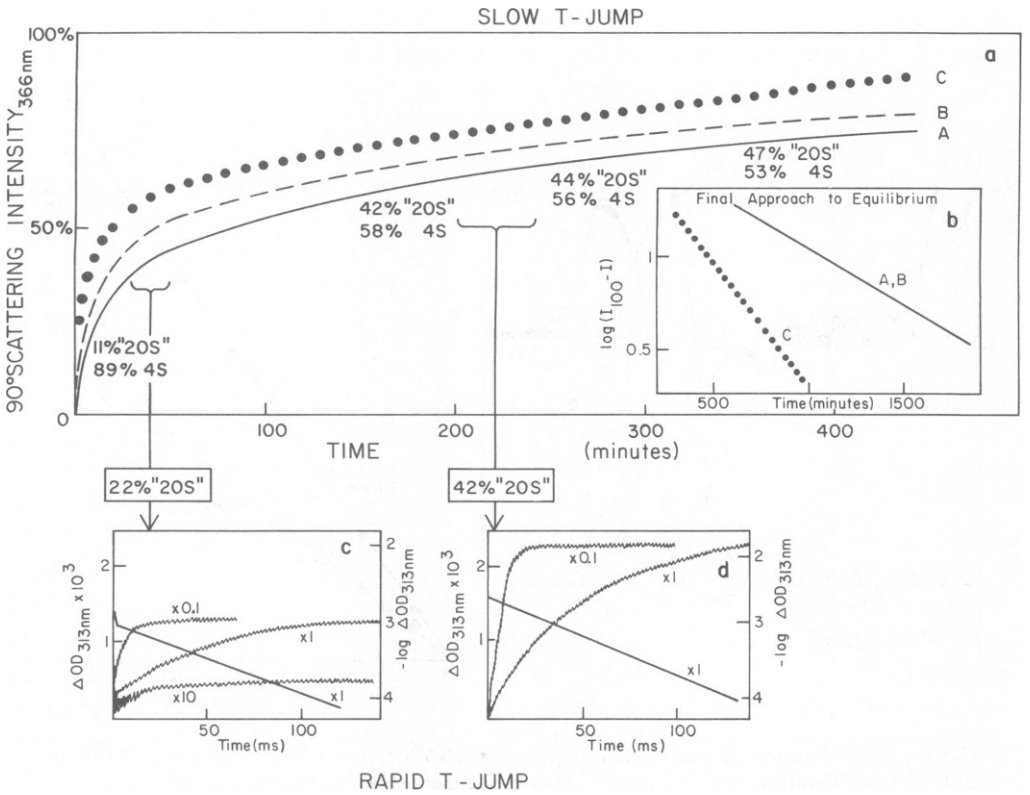

Figure 3 (*a*) Time-course of overall formation of "20S" protein measured by 90° light-scattering at 366 nm after slow temperature-jump (heating time 3 min) from 2 to 20°C at pH 7.00 ±.02°C using a modified Brice-Phoenix photometer (Phoenix Precision Instrument Div., Gardiner, N. Y.) and a 1-cm fluorescence cell with fused water jacket. Curve *A*: 3.8 mg ml^{-1} TMVP, 0.10 M *I* K(H)PO$_4$; curve *B*: 4.5 mg ml^{-1} TMVP, 0.027 M K(H)PO$_4$ + 0.0009 M cacodylate + KCl to give 0.10 M ionic strength; curve *C*: 0.02 M cacodylate + KCl to give 0.10 M *I*. Sample used for curve *A* was analyzed by analytical ultracentrifugation at 40 K rpm at various times to monitor formation of the "20S" boundary with the results shown beneath the kinetic trace. Special sample handling for sedimentation measurements is described in references 17 and 18. (*b*) First order kinetics plot for the slowest relaxation in "20S" formation, taken from the final approach to equilibrium in Fig. 3 *a*. curves *A*, *B*, $\tau^{-1} = 2.5\ (\pm 1) \times 10^{-5}\ s^{-1}$; curve, *C*, $\tau^{-1} = 5.5\ (\pm 1) \times 10^{-5}\ s^{-1}$. (*c*, *d*) Fast temperature-jump measurements (heating time 5×10^{-6} s) at two different "20S" protein concentrations, as measured during the course of "20S" formation shown in Fig. 3 *a*. Measurements were made in the forward scattered beam at 313 nm in a 1-cm quartz window cell with a 2°C temperature-jump starting at 18°C, using a dual beam, variable dynode optical system. (*c*) τ^{-1} (fast) $1 \times 10^{-3}\ s^{-1}$, τ^{-1} (slow) = 20 (±3) s^{-1}. (*d*) τ^{-1} (fast) amplitude too small to measure, τ^{-1} (slow) = 23 (±3) s^{-1}.

been given. The rate is very pH-dependent (R. B. Scheele, S. J. Shire, and T. M. Schuster, unpublished results), increasing over the pH range where the three-turn helix is formed (Fig. 1) to a half-time of < 30 min at pH 6.7 for 22S formation. At pH 6.5 helical TMVP rods consisting of over 1,000 subunits (about one-half the size of the whole virus) are formed from 4S protein within 1 min when warmed from 4 to 20°C (17). Thus the formation of helical polymers can be very rapid and it appears that slow steps are associated only with disk formation. The final approach to equilibrium during ~20S formation is exponential as is shown in Fig. 3 *b* where it is seen that at the two phosphate concentrations studied the rates are the same, 2.5 (±1) × $10^{-5}\ s^{-1}$ and about half as large as those obtained in non-phosphate

buffers, 5.5 (± 1) $\times$ 10^{-5} s^{-1}. This relaxation time appears to be nearly independent of 4S concentration as judged by an analysis of the time range over which the exponential fit extends in Fig. 3 *b* and by the fact that the relaxation time is essentially constant from 3–5 mg ml^{-1} total TMVP concentration. Since preliminary measurements (data not shown) indicate that the initial rate of ~20S formation does not appear to be rate limited by a conformation change, the relaxation rate expression for the final approach to equilibrium is expected to be of the form,

$$\tau^{-1} = f(k_i, k_i' C_{i \neq 20S}) + g(k_i'), \quad (1)$$

where f and g are functions which relate the normal reaction modes to the individual association rate constants, k_i, and dissociation rate constants, k_i'. From an analysis of the time range over which there is concentration independent relaxation to equilibrium in Fig. 3a, we estimate that at $c_{4S} \leq 2$ mg ml^{-1} the two terms in Eq. 1 are nearly comparable. Using the measured value of $\tau^{-1} = 2.5 \times 10^{-5}$ s^{-1} from Fig. 3 *b* we estimate a value of ~1×10^{-5} s^{-1} for the second term in Eq. 1. The existence of such a slow rate in the overall dissociation of ~20S is in accord with the very slow phase observed by Butler (26) in his dilution experiments and with our sedimentation measurements (S. J. Shire, J. J. Steckert, M. L. Adams, unpublished results) of the depolymerization rate of nearly pure ~20S protein prepared as in Fig. 4 *b*. Additional evidence for such a slow depolymerization rate of ~20S at pH 7.0 and 20°C comes from our virus reconstitution experiments (Fig. 5 *b*).

This analysis suggests that under conditions where both the rate of ~20S formation and the rate of virus assembly are often studied, the slow overall rate of ~20S formation may result from the fact that the slow back reaction, ~20S $\rightarrow$ 4S, becomes comparable in rate with the forward reaction rather early in the progress curve. This occurs because the rate of ~20S formation is strongly dependent on C_{4S} which decreases during polymerization.

When TMVP polymerization was studied by rapid temperature-jump relaxation methods at various times during slow ~20S formation, at the times indicated in Fig. 3, it was found that the turbidity changes between 5×10^{-5} and 2 s are well described by two relaxation processes, as shown in Figs. 3 *c* and 3 *d*. Our initial studies indicate that both of these millisecond processes are involved in polymerization. The amplitude of the slower relaxation increases with ~20S concentration, indicating that ~20S material is formed in this process. Similarly, as the 4S concentration decreases the amplitude of the faster relaxation decreases implicating it with reactions within the 4S distribution.

These preliminary rate studies of ~20S formation, from ~10^{-6} to 10^{+3}s, have revealed three resolvable relaxation processes and a submicrosecond conformation change, a relatively simple kinetic pattern considering the large number of elementary steps involved in ~20S formation. This pattern is not too surprising considering the lack of substantial concentrations of intermediates present at equilibrium, and suggests some highly cooperative processes, as has been proposed previously (22). However, before further progress can be made in understanding the elementary step kinetics of TMV assembly, a more quantitative characterization of the 4 to ~20S and 19–24S equilibria, and their protein coupling, will have to be completed.

MECHANISM OF ROD ELONGATION DURING TMV ASSEMBLY

Although the central role of ~20S TMVP in the initial interaction with RNA is generally agreed upon, there is a long standing controversy over the question of whether or not there is a

protein species which preferentially adds during the elongation phases of virus reconstitution (see references 4, 5, and 6 for detailed discussion of this controversy, as well as the following more recent papers: references 12, 27, and Butler and Lomonosoff, these proceedings.) To a large extent the controversy results from the fact that ~20S protein always exists as an equilibrium mixture with 4S aggregates and, with two exceptions (12, 28), all studies designed to determine the relative rates of ~20S and 4S incorporation during elongation have

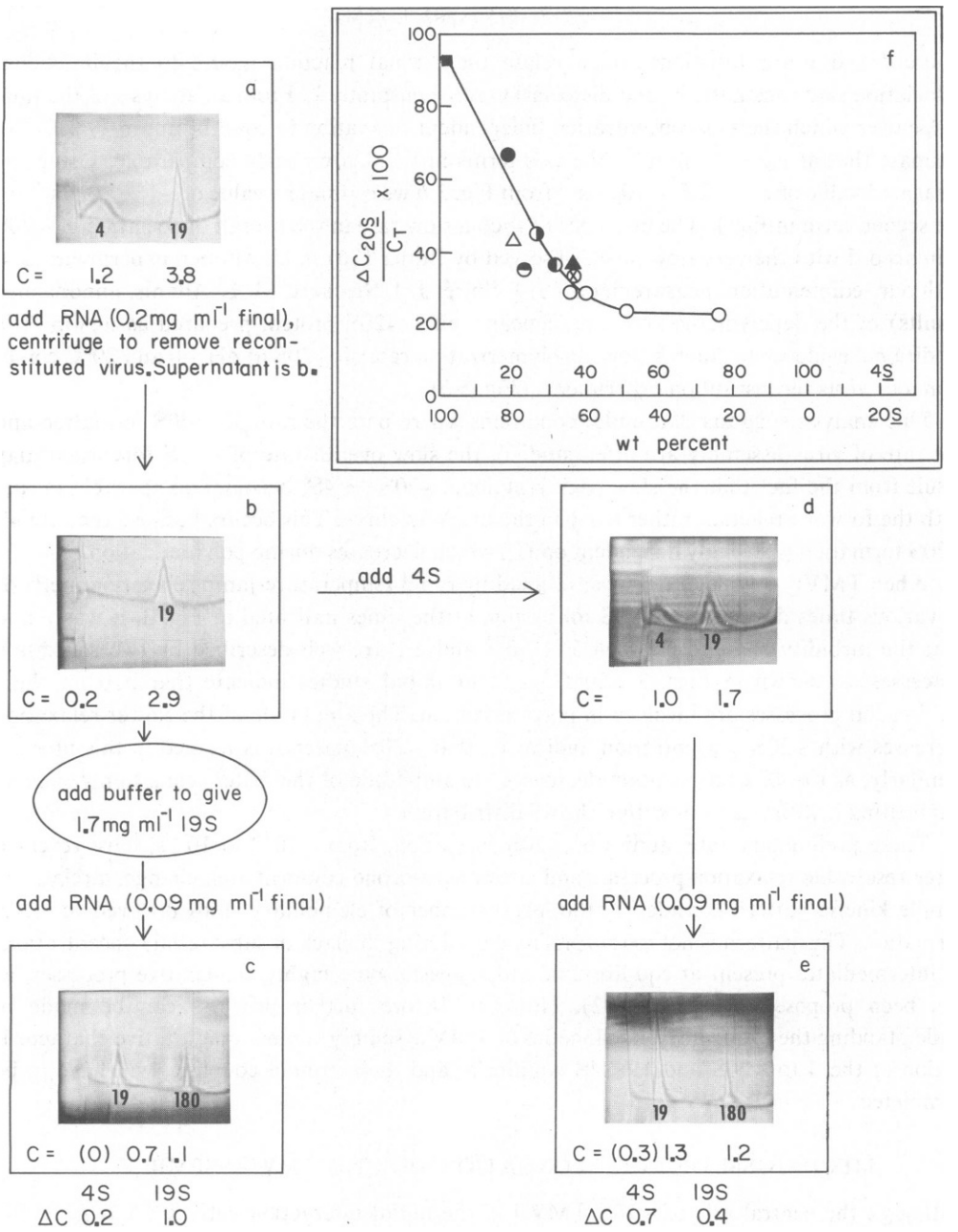

Figure 4

been based upon measurements by various means of the rates of appearance of reconstituted virus. Shire et al. (12) took advantage of a set of conditions where ~20S protein is metastable for very long times and does not interconvert with 4S protein, i.e., pH 6.5 and 6.5°C (18). Based upon direct measurements of rates of 4S and ~20S incorporation, using analytical ultracentrifugation, they provided evidence that during the elongation phases the 4S protein incorporates initially 50–70 times faster than the ~20S protein, although the latter is incorporated at longer times of reconstitution. Those studies also revealed two distinct kinetic phases for the elongation reaction, perhaps corresponding to the recently proposed bidirectional TMV assembly mechanism (29, 30). We have extended our reconstitution studies to conditions where the conflicting results from other laboratories have been obtained, pH 7.0 and 20°C. Since the dilution experiments of Butler (26) demonstrated a slow rate of ~20S depolymerization, we again used sedimentation analysis, as in the pH 6.5 and 6.5°C studies, to measure protein incorporation. The results of such experiments at pH 7.0 and 20°C are summarized in Fig. 4. The rates of ~20S depolymerization and formation are sufficiently slow under these conditions to make it possible to measure, within 20 to 30 min after RNA addition, the transient 4S and ~20S concentrations before the protein reequilibrates. However, the rate of virus reconstitution is too rapid to be measured in this way. Nevertheless, these transient concentrations should reflect the relative rates of incorporation of protein in the 4S and ~20S boundaries. In addition, turbidity methods were used to directly follow assembly kinetics, examples of which are shown in Fig. 5.

Fig. 4 *b* shows the transient protein composition obtained after adding RNA to a 5-mg ml^{-1} TMVP equilibrium mixture of 4S and ~20S protein shown in Fig. 4 *a*, the "disk preparation" of Butler (5). The 165S schlieren boundary representing the 2.1mg ml^{-1}, of reconstituted virus is not shown. Nearly all of the 4S protein, 1.0 mg ml^{-1}, was incorporated, whereas only ~24% of the ~20S protein, 0.9 mg ml^{-1}, was incorporated. The protein in the remaining supernatant solution is ~94% ~20S protein. This supernatant was then used for further virus assembly kinetics experiments, as shown. The supernatant ~20S protein was found to be fully capable of further reconstitution when an excess of RNA was added, resulting in complete elimination of the ~20S boundary (unpublished results). Mixtures with

Figure 4 (*a-e*) Sedimentation analysis of assembly of TMV at pH 7.0, 20°C in 0.10 M ionic strength potassium orthophosphate. Sedimentation coefficients are given on schlieren photographs for respective boundaries, and concentration of material in each boundary is given in mg ml^{-1} beneath each photograph. Details of sedimentation methods, special sample handling, protein and RNA preparations are given in references 12, 17, and 18. Photos were taken 20–30 min after each RNA addition. The time required to prepare solution b was ~45 min. All runs were at 40 K rpm in 12-mm double sector epon cells. RNA used for reconstitution sedimented with $s_{20,w}$ = 28S. The metastable ~20S supernatant, composition shown in Figure 4 *b*, depolymerizes slowly, $k \sim 1 \times 10^{-5}\ s^{-1}$, to the equilibrium distribution of ~2 mg ml^{-1} ~20S and 1 mg ml^{-1} 4S protein. (*f*) Weight percentage incorporation of ~20S TMVP $(\Delta C_{20S}/C_T) \times 100$, as determined by sedimentation analysis at different initial 4S to 20S TMVP weight ratios. All measurements were in 0.10 M *I* $K(H)PO_4$, pH 7.0 at 20°C. Three different methods were used to obtain the various initial 4S to 20S ratios. (*a*) TMVP solutions at 4.0 (▲), 4.9(◐), 5.1(◑), 6.8(●), 8.7(◓) and 8.9(Δ) mg ml^{-1} total protein were equilibrated > 24 h at 20°C and reconstituted with TMV-RNA at 0.20 mg ml^{-1}, except for 6.8 mg ml^{-1} sample where RNA was 0.27 mg ml^{-1}. (*b*) TMVP solutions at 4.6 mg ml^{-1} were equilibrated >24 h at 20°C then mixed in varying amounts with a 4.6 mg ml^{-1} TMVP solution just warmed from 0 to 20°C, containing only 4S protein to give various 4S to 20S ratios at 4.6 mg ml^{-1} total protein (O) and reconstituted with TMV-RNA at 0.20 mg ml^{-1}. (*c*) Supernatant ~20S protein was used to prepare TMVP solutions at 1.7 mg ml^{-1}(■) and 2.7 mg ml^{-1} (⊗) as shown in Figs. 4 *b* and 4 *d*. The solutions were then reconstituted with TMV-RNA at 0.09 mg ml^{-1} as shown in Figs. 4 *c* and 4 *e*. Initial 4S to 20S ratios were obtained from schlieren boundary areas of control protein samples run at the same time as the reconstituted samples, containing RNA. Formation and depolymerization of ~20S protein is negligible during the time of the experiment.

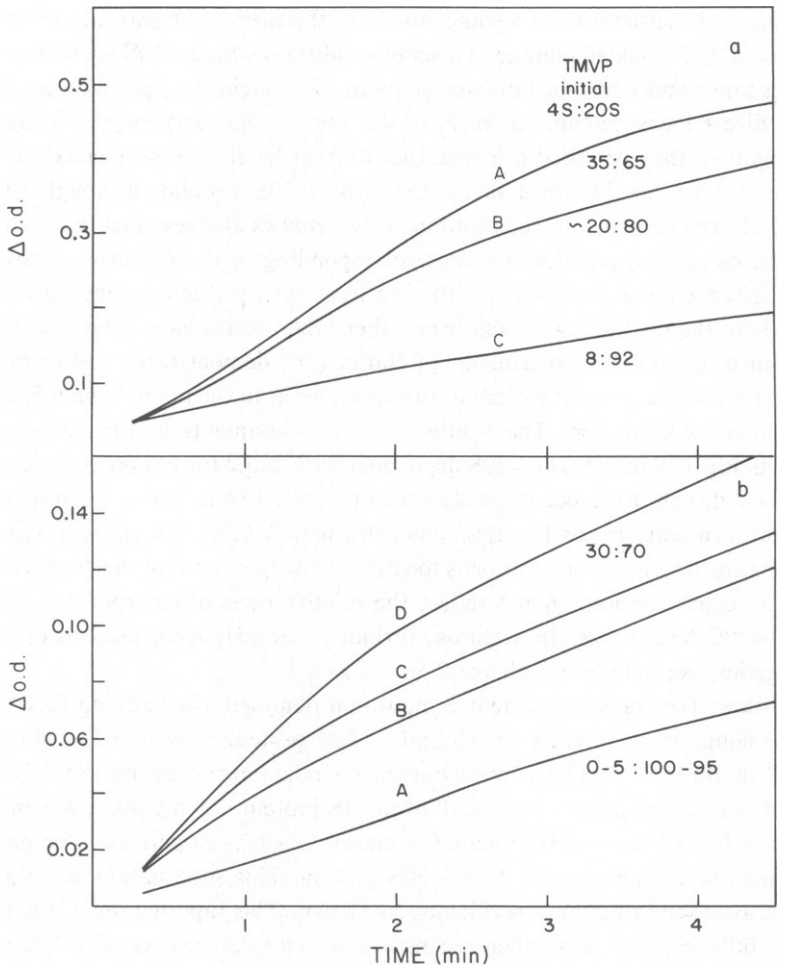

Figure 5 (*a*) Kinetics of TMV reconstitution at pH 7.0, 0.10 M *I* $K(H)PO_4$ as a function of initial mass ratio of ~20S to 4S. TMVP was 2.0 mg ml^{-1} and RNA was 0.1 mg ml^{-1}. Measurements of turbidity were made using a 0.1-cm thermostated cell at 310 mn in a Cary 118c spectrophotometer (Varian Instruments). Total dead time including RNA addition was 15–20 s. Solution compositions were determined by analytical ultracentrifugation as in Fig. 4. Protein samples were prepared as follows: curve *A*, a 5-mg ml^{-1} TMVP 20°C-equilibrated solution was diluted to 2.0 mg ml^{-1} and reequilibrated at 20°C for 15 h; curve *B*, a 10-mg ml^{-1} TMVP 20°C-equilibrated solution was diluted to 2.0 mg ml^{-1} just before addition of RNA; curve *C*, prepared as in Fig. 4 *b* but instead of removing reconstituted virus a second RNA addition was made to the first reconstitution mixture 20 min after the initial RNA addition. (*b*) Conditions as in *a*. Initial TMVP solution prepared as in Fig. 4 *b* to give 1.3 mg ml^{-1} TMVP. At various times during depolymerization to equilibrium, corresponding to increasing 4S to ~20S ratios at constant C_T, RNA was added to a final concentration of 0.11 mg ml^{-1}. Times, after the first RNA addition to produce 95–100% ~20S, when second RNA additions were made, were: curve *A*, 13, 25, 57 min traces all superimposable; curve *B*, 134 min; *C*, 200 min; curve *D*, 1,190 and 1,975 min, curves superimposable. Compositions of curves *A* and *D* were determined by analytical ultracentrifugation.

various ratios of 4S and ~20S supernatant protein were prepared using freshly warmed 4S protein which had not yet formed ~20S protein. The composition of one such mixture is shown in Fig. 4 *d*. An example of the solution composition after reconstitution using such mixtures is shown in Fig. 4 *e*. Shown in 4 *c* and 4 *e* are the results of a competition experiment in which, after dilution, the initial concentrations of ~20S protein before RNA addition were the same,

1.7 mg ml^{-1}. However, the initial concentrations of 4S protein in the two samples were 0.12 mg ml^{-1} in sample *b* and 1.0 mg ml^{-1} in sample *d*. Essentially the same concentration of reconstituted virus was produced in each case, 1.2 and 1.1 mg ml^{-1}. These results show for the first time that nearly pure ~20S protein (sample *b*) can fully participate in all phases of TMV reconstitution. It is not to be inferred from these results that a ~20S species is necessarily the aggregate that kinetically adds to the RNA. However, when 4S protein is also available to participate in the elongation reaction, as in sample *d*, only 40% of the amount of ~20S protein incorporated in sample *b* goes into the reconstituted virus. Electron microscope measurements of the reconstituted virus revealed no significant differences in the length distributions of the two reconstituted samples.

The results of similar reconstitution experiments using various initial ratios of 4S to ~20S protein are shown in Fig. 4 *f*. These different ratios of 4S to ~20S protein were obtained either by mixing 4S protein with ~20S supernatant or by diluting a high concentration of an equilibrium 4S:~20S mixture, as indicated in the figure. There does not appear to be any correlation with total initial TMVP concentration, but rather with the relative amount of 4S and ~20S protein present as can be seen by comparing the ~20S incorporation found using the 5.1 and the 8.9 mg. ml^{-1} protein samples. As the relative concentration of 4S protein is increased from ~5–50%, there is a near-linear decrease in the fraction of incorporated TMVP deriving from ~20S protein. The limited data beyond 50% 4S suggest that there is a region (or regions) of RNA (~1–1.5 kilobases) which preferentially (perhaps exclusively) binds ~20S protein. The steep initial slope in Fig. 4 *f* emphasizes clearly the sensitivity of the relative rates of incorporation, which this portion of the curve reflects, to exact temperature and pH conditions. Different laboratories have reported from ~80 to 65% ~20S, supposedly at pH 7.0, 20°C, 0.10 M ionic strength $K(H)PO_4$. According to Fig. 4 *f* this variation could result in a range of values for the percent of ~20S corresponding to 55 to 30%, respectively. Since the fraction and exact composition (Fig. 1 *a*) of the ~20S boundary are extremely pH- and temperature-dependent under these conditions, the observed relative incorporation rates of 4S and ~20S protein will also be rather sensitive to solution conditions.

Although these direct measurements of 4S and ~20S incorporation reflect relative rates, they do not provide kinetics data directly. The initial rates of turbidity change using TMVP solutions prepared as in Fig 4, are shown in Fig. 5 *a* for three 4S to ~20S ratios at constant TMVP and RNA concentrations. After an initial lag phase, corresponding to nucleation, there is a sharp increase in assembly rate with an increasing percentage of 4S protein. Another series of kinetics measurements was performed using a solution prepared in the same manner as the nearly 100% ~20S solution represented in Fig. 4 *b*. In this case RNA was added at various times to different portions of the slowly reequilibrating TMVP solution, which initially was 95–100% ~20S protein. It can be seen that as the ~20S protein depolymerizes to 30% 4S material, there is about a threefold increase in the initial rate of reconstitution at constant total protein concentration. It appears that the sedimentation results in Fig. 4 *f* agree with these results and do indeed reflect relative rates of ~20S to 4S incorporation, since there is about a 2.6-fold decrease in the relative amount of ~20S protein incorporated over the same range of 4S weight fraction used in the direct kinetics measurements, i.e., 5–30%

We have no single explanation for the apparently contrary results of Butler (references 28 and 32) and of Butler and Lomonosoff (31, see also these proceedings) who conclude that the rates of elongation are faster with "disk preparations" than with added 4S protein. It is important to note, however, that the methods used by Butler and by Butler and Lomonossoff

are less direct than those described here, in that their measurements depend wholly upon measurement and analysis of the products of the assembly reaction, whereas we have emphasized measuring directly the rates of incorporation of the reactants, i.e., 4S and ~20S protein. It is noteworthy that Butler has reported (32) the initial rate of assembly, as measured by turbidity changes, to be faster with added 4S protein than with "disk preparations" at low total protein concentrations. Under these conditions the relative concentration at equilibrium of 4S protein is greater than in "disk preparations" since C_{4S} does not depend on C_T as strongly as does C_{20S}, as first shown by Durham (25). We have redetermined this concentration dependence at pH 7.0, 20°C, 0.10 M ionic strength K(H) PO_4 and find

$$C_{20S} = 0.88\ C_T - 0.66$$

$$C_{4S} = 0.12\ C_T - 0.66$$

for C_T = 1 to 12 mg ml^{-1} (S. J. Shire and J. J. Steckert, unpublished results).

The data in Fig. 4 *f* suggest caution in interpreting experiments using prenucleated or partially assembled rods for studying the elongation, reaction since the overall process is clearly kinetically heterogeneous and thus sensitive to the initial degree of preassembly. It is a structural and thermodynamic intepretation of data, such as those in Fig. 4 *f*, which will illuminate details of the mechanism of TMV assembly

THE PROBABLE READING FRAME OF THE RNA AT THE NUCLEATION SITE FOR PROTEIN BINDING.

We have measured the binding of 25 different tritium labeled trinucleoside diphosphates to helical rods of polymerized TMVP (33) and compared these binding constants as a linear distribution along the known RNA sequence at the assembly nucleation site (34, 35). Details of these binding measurements will be published elsewhere (J. J. Steckert and T. M. Schuster, manuscript in preparation). The results indicate which of the three possible binding frames is the correct one for this highly specific protein–nucleic acid interaction. Trinucleoside diphosphates were chosen for study because of the known stoichiometry of three nucleotides per subunit in the intact virus. The proposed binding frame places two copies of the trinucleoside having the highest binding affinity of the 25 tested, AAG, sequentially adjacent to one another in the nonhydrogen bonded region of the folded RNA structure proposed by Zimmern and Butler (34). The proposed binding frame is based upon the following partial list of association constants measured at 20°C, pH 5.4, in 0.14 M KCl, 0.05 M acetate, 0.05 M $K(H)_2PO_4$:

5′ → 3′	$10^{-4} \times K\ (M^{-1})$
AAG	1.2
CAG	0.58
GAG	0.40
UAG	0.19
AUG	0.41
UGA	0.08
AGU	0
GAU	0
GAA	0.47

5′ → 3′	$10^{-4} \times K\ (M^{-1})$
AGA	0.10
AAA	0
GAC	0
UUG	0.12

We believe that the trinucleosides are binding at the RNA binding sites of the protein since no binding was detected using intact virus where those sites are occupied. Attempts to measure trinucleoside binding at pH 7.0 and 6.5, at 20°C, revealed very weak but measureable (K ~200–300 M^{-1}) binding by the same trinucleosides which show strong binding at pH 5.4

Briefly, these results show that (*a*) the affinity depends upon sequence and not composition (*b*) G in the 3′ position promotes binding, and (*c*) for the trimer XAG, the 5′ base influences binding in the order A>C>G>U>, (*d*) U or C in the 3′ position inhibits binding.

In the proposed binding frame the sequence -CAG-AAG-AAG-occurs at the nucleation site and, using the above binding constants, we expect a minimum of 10–14 kcal/mol of binding sites of binding free energy, without taking into account possible cooperative effects when binding as an intact RNA chain. Binding energies of this magnitude are to be expected for the high degree of specificity exhibited when ~20S protein selectively binds to the internal region on the RNA where assembly is initiated. Elucidation of the structure of the RNA binding region of the protein which binds some trimer sequences very strongly and yet can accomodate virtually all trimer sequences will probably reveal a subtle stereochemical basis for the selectivity of this specific protein-nucleic acid interaction which results in the initiation of virus assembly. A detailed description of this interaction may be available in the near future since significant progress has been made using x-ray diffraction methods in the determination of the structures of the two-layer disk aggregate of the protein (7) and of the intact virus (8).

The generous hospitality of The Johns Hopkins University Biology Department made possible the preparation and writing of this article.

These studies were supported by research grants from the University of Connecticut Research Foundation, the National Institutes of Health (NIH), (AI 11573), and by NIH National Research Service Award AI-05266 to Dr. Shire. Mr. Steckert is an NIH trainee.

Received for publication 20 December 1979.

REFERENCES

1. Fraenkel-Conrat, H., and R. C. Williams. 1955. Reconstitution of active tobacco mosaic virus from its inactive protein and nucleic acid components. *Proc. Natl. Acad. Sci. U.S.A.* **41**:690–698.
2. Caspar, D. L. D. 1963. Assembly and stability of the tobacco mosaic virus particle. *Adv. Protein Chem.* **18**:37–121.
3. Lauffer, M. A., and C. L. Stevens. 1968. Structure of the tobacco mosaic virus particle: polymerization of tobacco mosaic virus protein. *Adv. Virus Res.* **13**:1–63.
4. Richards, K. E., and R. C. Williams. 1976. Assembly of tobacco mosaic virus *in vitro*. *Comprehensive Virology*. H. Fraenkel -Conrat and R. R. Wagner, editors. Plenum Press, New York. **6**:1–37.
5. Butler, P. J. G., and A. C. H. Durham. 1978. Tobacco mosaic virus protein aggregation and virus assembly. *Adv. Protein Chem.* **31**:188–251.
6. Lebeurier, G., and L. Hirth. 1975. Le virus de la mosaique du tobac: Un modèle de morphogenese virale *in vitro*. *Bulletin de L' Institut Pasteur.* **73**:141–165.
7. Bloomer, A. C., J. N. Champness, G. Bricogne, R. Staden, and A. Klug. 1978. Protein disk of tobacco mosaic virus at 2.8Å resolution showing the interactions within and between subunits. *Nature (Lond).* **276**:362–368.
8. Stubbs, G., S. Warren, and K. Holmes. 1977. Structure of RNA and RNA binding site in tobacco mosaic virus from 4Å map calculated from x-ray fibre diagrams. *Nature (Lond.).* **267**:216-221.

9. Guilley, H., G. Jonard, B. Kukla, and K. E. Richards. 1979. Sequence of 1000 nucleotides at the 3' end of tobacco mosaic virus RNA. *Nucleic Acids Res.* **6**:1287–1308.
10. Ackers, G. K., and L. Katzel. 1979. The earliest stages of TMV-self-assembly. *J. Supramol. Struct.* **10**:216. (Abstr.).
11. Butler, P. J. G., and A. Klug. 1971. Assembly of the TMV particle from RNA and disks of protein. *Nature (Lond.). New Biol.* **229**:47–50.
12. Shire, S. J., J. J. Steckert, M. L. Adams, and T. M. Schuster. 1979. Kinetics and mechanism of tobacco mosaic virus assembly: direct measurement of relative rates of incorporation of 4S and 20S protein. *Proc. Natl. Acad. Sci. U.S.A.* **76**:2745–2749.
13. Durham, A. C. H., and J. T. Finch. 1972. Structures and roles of the polymorphic forms of tobacco mosaic virus protein. II. Electron microscope observations of the larger polymers. *J. Mol. Biol.* **67**:307–314.
14. Okada, Y., and T. Ohno. 1972. Assembly mechanism of tobacco mosaic virus particle from its ribonucleic acid and protein. *Mol. Gen. Genet.* **114**:205–213.
15. LeBeurier, G., and L. Hirth. 1973. Tobacco mosaic virus reconstitution at low ionic strength. *FEBS (Fed. Eur. Biochem. Soc.) Letters.* **34**:19–23.
16. Durham, A. C. H., J. T. Finch, and A. Klug. 1971. States of aggregation of tobacco mosaic virus protein. *Nature (Lond.) New Biol.* **229**:37–42.
17. Schuster, T. M., R. B. Scheele, and L. H. Khairallah. 1979. Mechanism of self-assembly of tobacco mosaic virus protein. I. Nucleation controlled kinetics of polymerization. *J. Mol. Biol.* **127**:461–486.
18. Shire, S. J., J. J. Steckert, and T. M. Schuster. 1979. Mechanism of self-assembly of tobacco mosaic virus protein. II. Characterization of the metastable polymerization nucleus and the initial stages of helix formation. *J. Mol. Biol.* **127**:487–506.
19. Shalaby, R . A. F., and M. A. Lauffer. 1977. Hydrogen ion uptake upon tobacco mosaic virus protein polymerization. *J. Mol. Biol.* **116**: 709–725.
20. Vogel, D., and R. Jaenicke. 1974. Conformational changes and proton uptake in the reversible aggregation of the tobacco mosaic virus protein. *Eur. J. Biochem.* **41**:607–615.
21. Durham, A. C. H., D. Vogel, and G. D. De Marcillac. 1977. Hydrogen ion binding by tobacco mosaic virus protein polymers. *Eur. J. Biochem.* **79**:151–159.
22. Butler, P. J. G., A. C. H. Durham, and A. Klug. 1972. Structures and roles of the polymorphic forms of tobacco mosaic virus protein. IV. Control of mode of aggregation of tobacco mosaic virus protein by proton binding. *J. Mol. Biol.* **72**:1–18.
23. Vogel, D. 1973. Evidence for a rapid structural change in TMV A-protein near neutrality. *Biochem. Biophys. Res. Commun.* **52**:335–341.
24. Herskovits, T. T. 1967. Difference spectroscopy. *Meth. Enzymol.* **11**:775–778.
25. Durham, A. C. H. 1971. Structures and roles of the polymorphic forms of tobacco mosaic virus protein. I. Sedimentation studies. *J. Mol. Biol.* **57**:289–305.
26. Butler, P. J. G. 1976. Assembly of tobacco mosaic virus. *Philos. Trans. R. Soc. Lond. B. Biol. Sci.* **276**:151–163.
27. Fukuda, M., T. Ohno, Y. Okada, Y. Otsuki, and I. Takebe. 1978. Kinetics of biphasic reconstitution of tobacco mosaic virus *in vitro*. *Proc. Natl. Acad. Sci. U.S.A.* **75**:1727–1730.
28. Butler, P. J. G. 1972. Structures and role of the polymorphic forms of tobacco mosaic virus protein. VI. Assembly of the nucleoprotein rods of tobacco mosaic virus from the protein disks and RNA *J. Mol. Biol.* **72**:25–35.
29. Butler, P. J. G., J. T. Finch, and D. Zimmern. 1977. Configuration of tobacco mosaic virus RNA during virus assembly. *Nature (Lond.).* **265**: 217–219.
30. Lebeurier, G., A. Nicolaieff and K. E. Richards. 1977. Inside out model for self-assembly of tobacco mosaic virus. *Proc. Natl. Acad. Sci. U.S.A.* **74**:149–153.
31. Butler, P. J. G., and G. P. Lomonossoff. 1978. Quantized incorporation of RNA during assembly of TMV protein disks. *J. Mol. Biol.* **126**:877–882.
32. Butler, P. J. G. 1974. Structures and roles of the polymorphic forms of tobacco mosaic virus protein. VII. Elongation of nucleoprotein rods of the virus RNA and protein. *J. Mol. Biol.* 82: 333–342.
33. Steckert, J. J., and T. M. Schuster. 1979. Recognition of trinucleoside diphosphates by helical rods of polymerized TMV protein. *J. Supramol. Struct.* **10**:217. (Abstr.).
34. Zimmern, D., and P. J. G. Butler. 1977. The isolation of tobacco mosaic virus RNA fragments containing the origin for viral assembly. *Cell.* **11**:455–462.
35. Zimmern, D. 1977. The nucleotide sequence at the origin for assembly on tobacco mosaic virus RNA. *Cell.* **11**:463–482.
36. Scheele, R. B., and M. A. Lauffer. 1967. Acid-base titrations of tobacco mosaic virus and tobacco mosaic virus protein. *Biochemistry.* 6:3076–3081.
37. Scheele, R. B., and T. M. Schuster. 1975. Hysteresis of proton binding to tobacco mosaic virus protein associated with mestastable polymerization. *J. Mol. Biol.* **94**:519–525.

DISCUSSION

Session Chairman: Victor Bloomfield *Scribe*: Jonathan B. Chaires

BUTLER: I am unhappy with the design of the experiment shown in Fig. 4. You have demonstrated that the 19–20S peak is a very heterogeneous mixture of aggregates, yet after you deplete the mixture by reaction with RNA, you use the residual mixture as if it were the same material as you had before. You then go on to do elongation measurements and add more A-protein (4S protein) to the mixture. If certain of the species present in that original boundary are preferentially adding to the RNA, you will have depleted your supply. Therefore, you have a problem of interpreting what happens subsequently.

SCHUSTER: In the first place, if we add an excess of RNA, all of the protein is incorporated. Secondly, referring to Fig. 4, the first observation going from the left hand panel down represents the addition of RNA and the preferential removal of 4S protein. We have started with equilibrium protein—your so-called disk preparation—the same mixture you have used in your reconstitution experiments. We have simply put this into the centrifuge to see which species are incorporated.

SHIRE: Furthermore, in the reconstitution experiments, we didn't use only supernatant 20S protein to make our non-equilibrium mixtures; we also used equilibrium protein with 4S protein added. The reconstitution with these protein samples is also included in Fig. 4.

BUTLER: The trouble is, whenever you let things run down in the mixture of aggregates of the protein you may be depleting the critical component from the 20S boundary. I'm not saying that you've got to run it right down; it's better to work at the highest rates we can get so as to offer the system a choice.

Another point. You say that you absolutely require disk addition for ~1.5 kilobases. We get a minimum measured length of 2.25 kilobases. I don't see any simple reason why you should use that aggregate up to that length and then stop abruptly. We both would agree that it's too long simply to be the minor tail. But you've not gone far enough. You've just reached the point where you've pulled the end of the longer tail up into the center of the hole of the growing rod. You need to have some switching mechanism to change over the mode of assembly very dramatically at a point without any obvious signpost. It's not clear to me how you'll do that simply.

SCHUSTER: You are trying to interpret these results in the framework of a model that is not fully tested and which does not take into consideration other possible RNA secondary structures beyond what we know is important for nucleation alone. We have to proceed the other way around, and go from the observations to a test of the assembly model, and to a possible refinement of it.

J. KING: I want to second the point that inside the cell the RNA has functions other than to serve as a model for biophysicists studying assembly. It is perfectly reasonable to think there are features of the secondary structures that have not evolved to make assembly smooth and which therefore provide singularities in the assembly process. You mention the experiments of Stussie, LeBeurier, and Hirth where they show that 1/3 of the way up the TMV there's something special. I am absolutely unclear what that might be. We must assume that there are aspects of secondary structure unrelated to assembly that may produce singularities in the assembly process.

BUTLER: That's 1/3 up the TMV to go, so it shouldn't be confused with 1,500.

HENDRICKSON: Whatever the mechanism is, it seems to be more complicated that one might expect. We'll have to have different mechanisms for elongation in two different directions. From arguments of efficiency, it seems one would like fewer or more elegant alternatives. Is there any reason why growth has to start somewhere other than at the beginning? Why does it start at 1/6?

SCHUSTER: I can't say that it is exactly 1/6; our data do show that it's internal.

To see this you have to inquire into the origin of the specificity. Recall that Jo Butler mentioned that the stoichiometry of binding is 3 nucleotides per subunit. It's a very good number.

John Steckert has interrogated the sequence basis of this specificity by synthesizing a large number of trinucleoside diphosphates and measuring their binding constants to the preformed, helical rods. Control experiments show that they are not binding at adventitious sites. We get the same binding constants whether we allow the helix to form in the presence of these trinucleotides or when the nucleosides are added to preformed helices. What is shown in the table in our paper is that, although the binding constants are not strong, there is considerable discrimination (see reference 33).

If you consider the possible implications of this in terms of the number of sequential pairs of triplets having binding constants greater than, say, 10^3 or 10^4 M_1, you find that one particular binding sequence stands out: the sequence shown by Jo Butler and determined by Zimmern (see references 34 and 35).

If we add this up without considering cooperative effects we find that the CAGAAGAAG region at this loop contributes between 10 and 14 kcals of binding energy. This is the sort of number one would like to have for a specific interaction. One of the ways to ensure that this kind of site is available for nucleation, and not folded, is to put it into a loop region. It has to be internal in order to be in a looped region. This is, of course, only an *ad hoc* explanation.

HENDRICKSON: But why does it have to be so entirely internal?

SCHUSTER: There is almost certainly a regulatory function to this structural feature. You're asking why it is 1,000 nucleotides in rather than 10 or 20. I think that has something to do with the coordinated regulation between assembly and protein synthesis. Perhaps Jo Butler can comment on that.

BUTLER: There is a side of this that is not biophysics but plant pathology. The coat protein cistron—the viral genome—is the region we're talking about. We're dealing with a eucaryotic protein synthesis system where you cannot translate a polycistronic messenger. The only cistron that can be read has a premature terminating point. Two large protein products are made which have the same amino acid sequence up to termination. They're in the same place for nucleation. There's also a middle cistron which we know about, and a coat protein cistron. The cleavage site which you would require to generate this mRNA happens to be blocked by the nucleation site. So it may very well be a mechanism whereby the virus has evolved to prevent cleavage of these molecules it's already packaging. There are other strains of TMV where the coat protein message does get coated. On the whole, they make less virus in the plants, and don't grow as efficiently as the wild type.

If I might make one point on specific interaction: I misunderstood Schuster's terminology about the "reading frame" corresponding to the subunit boundaries. When we in Cambridge looked at the sequence of the origin of assembly on the RNA, we couldn't decide where the subunit boundaries would be with respect to that sequence. I accept the data that the particular trinucleotides with the hydroxyls at the ends are the favored ones for binding to a continuous protein aggregate, but you cannot tell the place with respect to the protein from any continuous aggregate because it must span protein gaps.

SCHUSTER: I agree. In fact, there is reason to think that the tight binding sequence might bridge subunits, thereby providing a means of stabilizing the helical structure.

J. KING: Obviously, the only way this whole thing can work is if the protein—the A-protein, the disk—does not bind to RNA at the non-nucleating sequence, which goes back to this question of the regulation of assembly. What about the binding of any form of the protein to other sections of the RNA? It seems to me that the protein in solution does not bind RNA spontaneously. It has to be incorporated into the rod to be activated for that. If not, you would see that stuff, coming off and going on all over the molecule. Has any one quantitated the binding with the nucleation segment gone?

SCHUSTER: Not that I know of.

J. KING: What about a rough approximation? What is the strength of binding to the non-nucleation segment?

SCHUSTER: There are some published Japanese electron micrographs that show in already-nucleated rods the tail region slightly decorated with subunits, but in a scattered fashion.

J. KING: Which tail?

SCHUSTER: I don't think we can tell from these early micrographs. You would expect not to find it, in fact, for the very reasons you presented earlier for bacterial flagellin. If you want a system that's regulated, you want a nucleation-controlled system. Here the nucleation is on the surface of the RNA. This provides the opportunity to have what corresponds to a super-saturated solution in the protein alone when you raise the temperature or lower the pH.

J. KING: So in fact this behaves as though you don't see binding between the free protein and random stretches of RNA. The reason we haven't seen numbers is that people were hitherto embarrassed by that observation, or didn't think it was important.

BUTLER: You can drive in other sections of broken-up RNA, by forcing the conditions a bit. You can certainly get binding of a major site within the coat protein cistron. People have drawn the parallel between that and the the binding site in the cowpea strain. You do have to push up the ionic strength. Atabekov's data show that when you

chop the RNA into shorter and shorter pieces suddenly you go from one binding site per intact molecule to several, so it may be that short lengths can bind less specifically. However, the data strongly suggest that in the long intact RNA is the only unique site.

SCHUSTER: That certainly implies that the secondary structure of the RNA may be such that it inhibits nonspecific binding.

GAREL: If I understand the argument, Dr. Butler is arguing from data on the rate of assembly vs protein concentration that the disk is preferentially adding during elongation, while Dr. Schuster maintains that the A-protein is adding on by examining the species remaining after completion of the process. It seems to me that these are different kinds of measurements. In such a complex process, can one not accommodate both kinds of data?

SCHUSTER: It is hard to know exactly what the microscopic adding species is. We have done rate studies under conditions where we can really measure the rate of incorporation of the reactions *per se* in the centrifuge. We find that the A-protein, on a molar basis, is incorporated at pH 6.5 and 6.5°C some 50–70 times faster (see reference 12).

I want to emphasize something related to Lee Makowski's comment, that there may be more than one way to reconstitute the virus.

From the point of view of an in vivo experiment, a tobacco leaf lives in a temperature range of 20–40°C over the course of 24 h. A 20–40°C spread would put most physical chemists out of business with this protein. This past week, Mary Adams followed the temperature dependence of reconstitution at pH 7.0 by 90° scattering. She saw a change not only in the initial rates but also in the shapes of the progress curves.

Similarly, there is a significant pH dependence of this reaction at 20°C.

I'm not suggesting that the pH of a plant cell changes very much, but it certainly is true that the temperature must change and this means that there must have been some sort of molecular adaptation to account for this and still produce viable virus. We know that the TMV infection is so effective in the plant cell and becomes so concentrated that you actually get liquid crystals, with TMV particles lining up in enormous concentrations.

GAREL: Are you and Dr. Butler looking at the same process? The same pathway?

SCHUSTER: We have carried out no experiments with partially assembled rods. We have carried out all of our experiments with naked RNA so that we could see the entire course of the reaction. What we found is that there is a small number of disks incorporated in a burst followed by a major incorporation of the 4S protein. We've done this under conditions where Butler has studied the elongation reaction.

HARRISON: A point of information. You speak of the addition of 4S protein. My understanding is that the 4S protein is primarily trimer. My own picture of the trimer would involve at least 4 states: 1 in the top and 2 in the bottom or 2 in the top and 1 in the bottom of each disk-like or helix-like aggregate. In fact, when you speak of 4S protein, what are you actually imagining?

SCHUSTER: What I'm imagining is that monomers may add. We know that there is a rapid monomer–trimer equilibrium which has been characterized with a very high degree of accuracy by Les Katzel and Gary Ackers. When we go to higher concentrations where we have trimer and, say, disk present, temperature-jump experiments show that there is a 1 ms event which corresponds to polymerization, which is most likely the addition of a monomer or something very small. So I'm not constrained by the structure of the trimer when I think of the species that is adding.